Hypersonic Viscous Flow Over Slender Cones†

L. TALBOT,* T. KOGA,** AND P. M. SHERMAN***

University of California at Berkeley, and University of Michigan

Summary

Viscous self-induced pressures on 3° semivertex angle cones were measured over the Mach Number range $3.7 < M_1 < 5.7$, and for values of the viscous interaction parameter in the range $0.5 < \bar{\chi}_c < 2.3$. The data were found to be in good agreement with results obtained by Talbot on 5° cones in the range $3.7 < M_1 < 4.1$, $0.9 < \bar{\chi}_c < 3.6$. All these data were correlated reasonably well by the viscous interaction parameter.

A new method for calculating self-induced pressures is presented which takes into account the interaction between boundary-layer growth and the inviscid flow field at the outer edge of the boundary layer. Pressures calculated by this method were only 10 to 20 per cent higher than the measured values.

Symbols

C = Chapman-Rubesin factor in relation $(\mu/\mu_2) = C(T/T_2)$
d = diameter of pressure orifice
K_c = similarity parameter, $M_1\theta_c$
K_2 = similarity parameter, $M_1\theta_2$
M = Mach Number
p = static pressure
r_c = cone radius
Re = Reynolds Number
t = bluntness of cone tip or thickness of leading edge of plate
T = gas temperature
u = gas velocity
x = distance measured from vertex along cone surface
y = distance normal to cone surface
γ = specific heats ratio
δ^* = boundary-layer displacement thickness,

$$\int_0^\infty [1 - (\rho u/\rho_2 u_2)]dy$$

δ = boundary-layer thickness
μ = absolute viscosity
ν = kinematic viscosity
ρ = gas density
σ = Prandtl Number
Λ = mean free path
θ_δ = streamline inclination at outer edge of boundary layer
θ_c = cone semivertex angle
θ_2 = $\theta_c + \theta_\delta$
$\bar{\chi}_c$ = viscous interaction parameter, $M_c^3(C/Re_{x_c})^{1/2}$

Subscripts

1 = free-stream conditions
2 = conditions at outer edge of cone boundary layer, taken to be functions of x
c = ideal flow conditions along surface of cone obtained for $x \to \infty$
w = wall conditions
aw = adiabatic wall

Examples of the notation used for the various Reynolds Numbers are: $Re_2/\text{in.} = u_2/\nu_2$, $Re_{t_1} = u_1 t/\nu_1$, $Re_{x_c} = u_c x/\nu_c$, etc.

Introduction

The fluid-dynamic and thermodynamic phenomena associated with flight at hypersonic speeds have been the subject of intensive research in recent years. In this research one problem that has received considerable attention is the problem of the "self-induced pressure" effect, which is one aspect of a broader class of phenomena which can be described as "viscous interaction" phenomena.

Although the fundamental mechanism responsible for self-induced pressures is well understood, the analysis of the effect is rather complicated. The magnitude of the self-induced pressure is directly proportional to the rate of growth of the boundary layer. (See Fig. 1.) However, the growth of the boundary layer is determined by the pressure, Mach Number, etc., in the flow at the outer edge of the layer, and the values of these quantities depend on the magnitude of the displacement effect. It is seen, therefore, that we have to deal with a complex interaction phenomenon in which the boundary-layer "history" plays an important role. It will also be recognized that the phenomenon is, with regard to magnitude, more significant for thin bodies such as flat plates and slender cones than for thick bodies, since for thin bodies the changes in effective geometry due to boundary-layer growth will be proportionately larger.

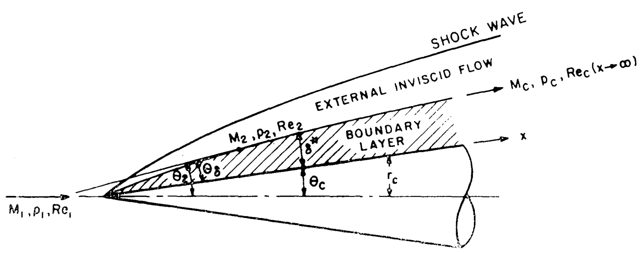

FIG. 1. Schematic of viscous flow over a cone.

Presented at the Aerodynamics—I Session, IAS 27th Annual Meeting, N.Y., Jan. 26–29, 1959.

† This work was sponsored by the National Advisory Committee for Aeronautics. An extended version is contained in NACA TN 4327.

* Associate Professor of Aeronautical Sciences, University of California, Berkeley.

** Professor of Engineering, University of Nagoya, Japan. Visiting Professor of Aeronautical Sciences, University of California, Berkeley, July-December 1956.

*** Research Engineer, University of Michigan, Ann Arbor.

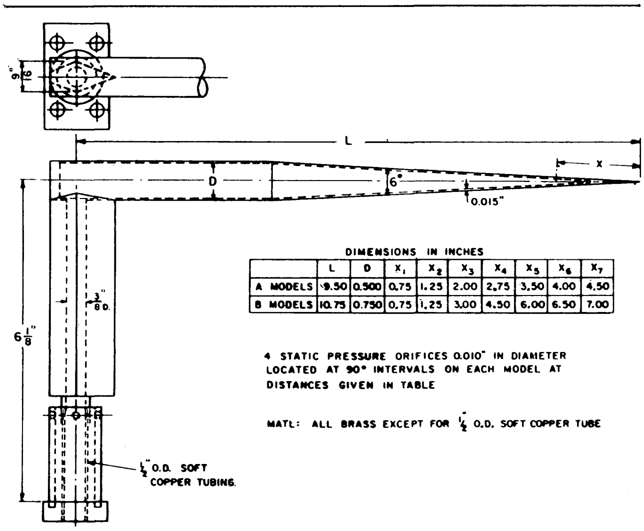

FIG. 2. Model specifications.

The particular problem considered in this paper is the self-induced pressure effect on a slender cone. In the first part of the paper new data are presented for pressures on 3° semivertex angle cones in the range of flow conditions $3.7 < M_1 < 5.8$; $650 < Re_{x_1} < 32{,}000$. Theories used for comparison with experiment are presented in the Appendixes.

Previous Experimental Results

The only data which have been available up to now for the viscous interacting air flow over a cone are the experiments of Talbot[1] and Baldwin.[2] Talbot's results were obtained in the Low Density Wind Tunnel of the University of California, the same wind tunnel used for the present work. His tests were carried out on 5° semivertex angle cones, in the Mach Number range $3.7 < M_1 < 4.1$, and at Reynolds Numbers which corresponded to the viscous interaction parameter range $0.91 < \bar{\chi}_c < 3.54$. Baldwin's data were obtained in the GALCIT 5″ × 5″ Hypersonic Wind Tunnel, Leg No. 1. His data were also for a 5° cone, at $M_1 = 5.8$, and over the viscous interaction parameter range $0.1 < \bar{\chi}_c < 1.6$.

Description of Present Experiments

Wind Tunnel

The experiments were conducted in the No. 4 Low Density Wind Tunnel of the Low Pressures Project of the University of California. This wind tunnel, which is an open-jet continuous-flow type employing axially symmetric nozzles, is described in detail elsewhere.[3] Two nozzles were used in the tests: the No. 8 nominal Mach 4 nozzle which produces flows in the range $3.7 < M_1 < 4.1$, $90 < Re_1/\text{in.} < 3{,}600$, and the No. 9 nominal Mach 6 nozzle, which produces flows in the range $5.5 < M_1 < 5.8$, $4{,}000 < Re_1/\text{in.} < 9{,}000$. Actual values of the flow parameters obtained in the test are listed in Table 1.

TABLE 1
Flow Conditions of Tests, $T_0 = 300°K$.

M_1	p_1 (μHg)	Re_1/in.	p_c/p_1 ($\theta_c = 3.03°$)
3.70	49.8	880	1.106
3.91	73.0	1,510	1.114
3.97	85.1	1,860	1.117
4.05	108.8	2,540	1.120
5.47	66.5	4,530	1.207
5.73	113.3	8,980	1.223

Models

All the cones tested were of 3° semivertex angle. Two sets of models were used, each set consisting of seven cones (see Fig. 2). The Type A cones had base diameters of 0.500 in., and the Type B cones had base diameters of 0.750 in. The longer Type B models were designed primarily to investigate the influence on the cone surface pressure of the expansion wave generated at the juncture of the conical surface and the cylindrical afterbody. Alignment of the cones in the flow was accomplished by adjustable set screws in the base support.

Subsequent to its use in the pressure measurement tests, Model B-7 was fitted with four copper-constantan thermocouples soldered in the cone surface at 2, 3, 4, and 5 in. from the vertex. This model provided information on the wall temperature of the cones, which was required for the boundary-layer calculations.

Some difficulty was encountered in producing models with sharp tips. The method of fabrication which was found most satisfactory was an acid etching process. After the cones had been machined to nearly their final dimensions, the tip regions were etched by a flat tool covered with a thin film of nitric acid. This method produced tips with diameters less than 0.001 in. However, the etching was not completely uniform. In the etched regions of the models, which extend back from the vertices about 0.4 in., some local variations in cone angle of several degrees were observed. Further back from the vertices all cone angles were found to be 3.03° ± 0.03°.

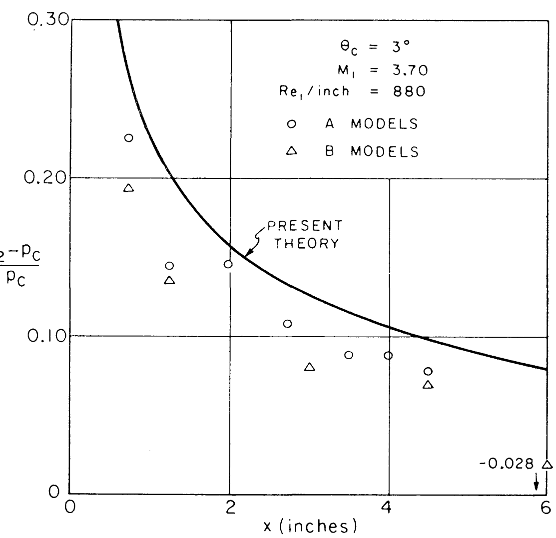

FIG. 3(a). 3° cone data, $M \sim 4$.

Instrumentation

Cone surface pressures were measured with a temperature-regulated thermistor manometer. The least count (0.1 mv) of the potentiometer used to measure the bridge unbalance of the thermistor measuring circuit corresponded to a pressure increment of about 0.02 micron Hg. Before each test the thermistor was calibrated statically against a precision McLeod gage. Analysis of the thermistor calibration data yielded a probable error in absolute pressure of about 1 per cent.

Wind-tunnel stagnation pressures were measured with a mercury manometer. Impact pressures were measured with a butyl phthalate oil manometer. Both manometers were equipped with magnifying optics which made it possible to locate the menisci to within 0.001 in.

Nozzle Calibration

Mach Numbers and static pressures in the test regions of the nozzles were determined by measuring stagnation and impact pressures, assuming the flow to be isentropic. For each flow condition of the tests, an axial impact pressure survey was made to determine the Mach Number and static pressure variations in the regions occupied by the models.

The tunnel-empty traverses in the No. 8 nozzle revealed a region about 8 in. in axial extent over which the Mach Number variation was less than 2 per cent and the static pressure variation less than 10 per cent. In the No. 9 nozzle the axial extent of the region over which the Mach Number and static pressure variations were less than these values was about 3.5 in.

Procedure

In the tests reported, all models were positioned so that their vertices were located at the same point in the flow. Correction was made for the axial gradients. Other tests were made with models positioned so that their respective pressure orifices were at the same axial location in the stream. The surface pressures obtained by this second method agreed quite well with those obtained by the first method. The correction for axial gradients in the stream was accomplished simply by using the local Mach Number (from tunnel-empty measurements) in the determination of the inviscid cone pressure p_c. It was found that this procedure gave consistent results provided the static pressure in the flow at the point where orifices were located did not differ by more than about 10 per cent from that at the vertex of the model. Consequently, in the No. 9 nozzle where the length of usable flow was about 3.5 in., models for which $x = 3.5$ in. were not used in the final tests. No difficulties arose on this score in the No. 8 nozzle. However, it was observed that the expansion wave reflection of the bow shock (the reflection occurring in the region of strong density gradient where the isentropic core merged with the nozzle boundary layer) affected the pressures measured on models B-6 and B-7. For this reason data are not reported at $M \approx 4$ for these models.

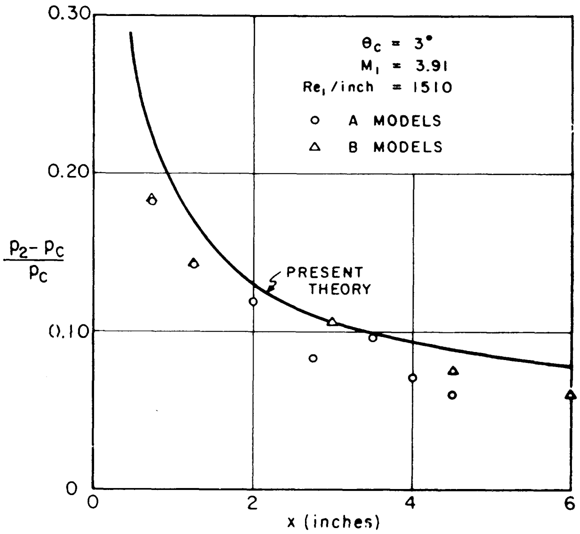

FIG. 3(b). 3° cone data, $M \sim 4$.

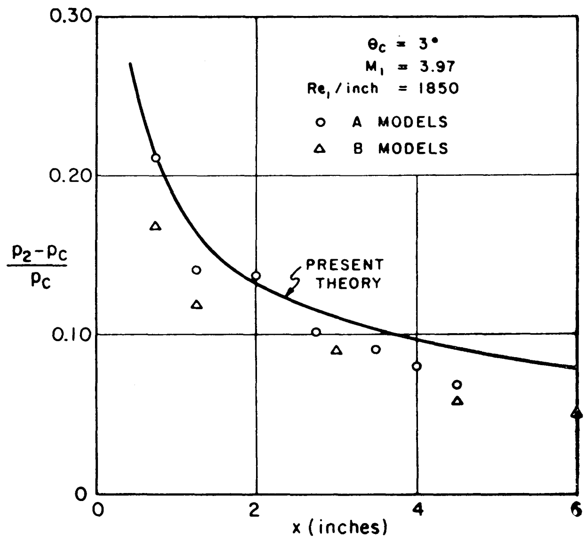

FIG. 3(c). 3° cone data, $M \sim 4$.

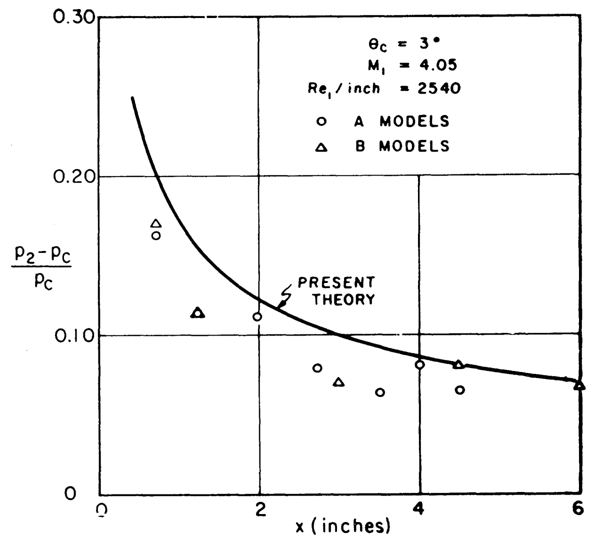

FIG. 3(d). 3° cone data. $M \sim 4$.

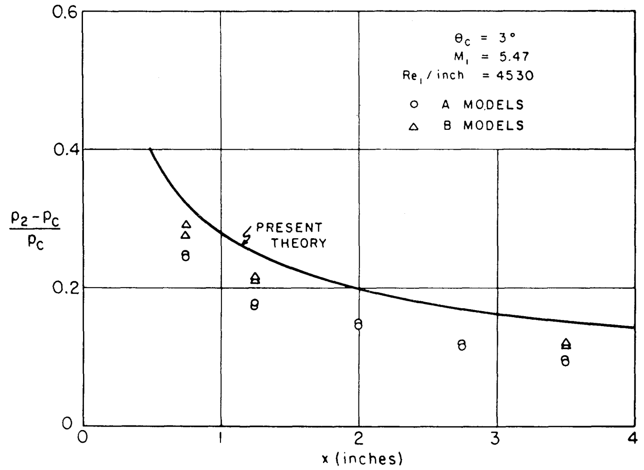

FIG. 4(a). 3° cone data, $M \sim 6$.

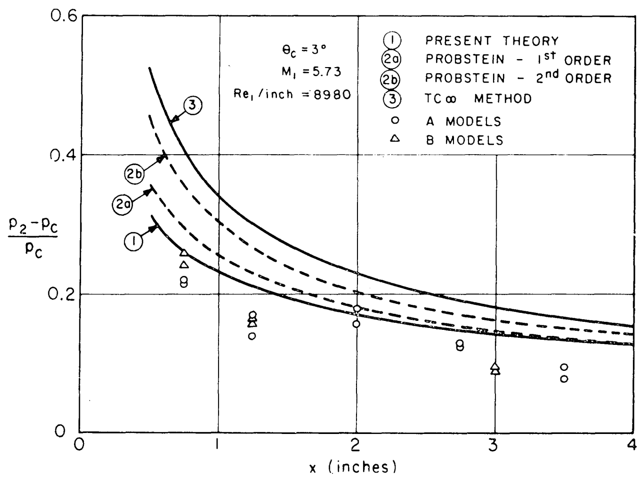

FIG. 4(b). 3° cone data, $M \sim 6$.

The temperature measurements made with Model B-7 showed the surface of the cone to be isothermal. The apparent recovery factor (based on inviscid flow conditions M_c, T_c behind the conical shock) was about 0.89; the increase over the theoretical value of 0.85 for the laminar boundary layer is due to heat conduction through the support from the model mounting, which was at essentially stagnation temperature.

Results

Results of the tests are given in terms of the induced pressure increment $p_2/p_c - 1$, where p_2 is the measured cone pressure and p_c the inviscid Taylor-Maccoll value. The inviscid flow values for the 3° cones were calculated from Van Dyke's second order theory,[4] since interpolation in the Kopal Tables[5] between 0° and 5° was not sufficiently accurate. The data at different flow conditions are shown plotted versus x in Figs. 3 and 4, and in Fig. 6 versus the hypersonic similarity parameter $\bar{\chi}_c = M_c^3(C/Re_{x_c})^{1/2}$ where M_c and Re_{x_c} are the Mach Number and Reynolds Number based on ideal Taylor-Maccoll flow conditions.

Numerical values for the induced pressure increment are in the range 0.06–0.30. The actual measured cone pressures varied between about 60 and 170 microns Hg. An error of 1 per cent in the measured pressure is equivalent to an error in the induced pressure increment of 5 per cent or more for most of the data, assuming the values of p_c to be exact, and from this it is estimated that the overall probable errors in $p_2/p_c - 1$ are between 5 and 15 per cent. Free-stream Mach Numbers are accurate to about 1 per cent; free-stream Reynolds Numbers are accurate to about 5 per cent.

In addition to the results of the present tests, two sets of data taken from reference 1 are shown in Fig. 5. In Fig. 6 all of the data from reference 1 on models A-1 through A-7 are plotted, and also Baldwin's 5° cone data are represented by a single line.

Discussion

Experimental Results

One conclusion which can be drawn from an examination of Figs. 3 and 4 is that the effect of the shoulder expansion did not extend far enough upstream in the cone boundary layer to influence the cone surface pressures, since the data obtained with the B models agree, within experimental scatter, with those obtained with the A models. We were not able to determine the extent of the region on the cone which is influenced by the shoulder expansion, because the reflection of the bow shock wave back onto the models obscured the effect. Models B-6 and B-7, which were designed to measure upstream influence, were those most affected by the reflected wave. In Fig. 3(a) it will be noted that the pressure orifices on model B-5 were also within the zone influenced by the reflection.

The scatter in the data is probably due to a combination of experimental error, imperfections in the orifices, and inaccuracies in the cone angle in the tip regions of the models. One may note that the reproducibility of the data was quite good, as evidenced by the comparisons shown in Figs. 4(a) and 4(b) between different sets of measurements made with both the A and the B models.

It can be seen from Fig. 6 that the parameter $\bar{\chi}_c$ provides a fairly good correlation for all of the data obtained in the University of California Low Density Wind Tunnel. The Mach 4 data for the 3° and 5° cones agree quite well; the Mach 6 data are slightly lower.

It is also seen from Fig. 6 that the induced pressure increments found by Baldwin are higher by a factor of about 2 than those obtained here. One suggestion which has been advanced is that the differences may be due in part to the influence of tip bluntness. It is true that the Reynolds Numbers based on tip diameter were higher in Baldwin's experiments than in ours; Baldwin's were mostly in the range $65 < Re_{t_1} < 230$, whereas all the Low Density Wind Tunnel data correspond to $Re_{t_1} < 9$. However, it seems unlikely that tip bluntness could account for much of the difference. The experiments on flat plates[6, 7] indicate that below about $Re_{t_1} = 80$ the plate can be considered as "sharp," and the effect of tip bluntness has been shown to be much less pronounced for cones than for flat plates.[8]

Comparisons Between Theory and Experiment

Three methods for calculating self-induced pressure have been employed in this report. The first, a new method devised by us, is presented and discussed in Appendix (A). The second, a method proposed by Probstein, is reviewed in Appendix (B), as is the third, which we have called the "TC_∞" method.

Figs. 3, 4, and 5 show that the present method for calculating self-induced pressures generally overestimates the data obtained in the Low Density Wind Tunnel by about 10–20 per cent. In contrast, the TC_∞ method and the Probstein second-order theory both give values greater by about a factor of 2 than the experimental results. The better agreement obtained with the present method is not surprising. Of the three methods it is the only one which accounts in even an approximate way for the true interaction effect, wherein the changes in the external flow due to the presence of the boundary layer feed back into the layer and alter its rate of growth. It seems likely that the discrepancies remaining between experiment and theory may be due mainly to the transverse curvature effect. [See Appendix (A).]

In Fig. 6 the results of the present theory are represented by a single straight line. (Actually, the individual curves of Figs. 3, 4, and 5 when plotted against $\bar{\chi}_c$ deviated about ± 2–4 per cent from this mean line. The deviations seemed not to follow any particular trend, and were probably due mainly to accuracies introduced in the graphical parts of the analysis.) Again, in Fig. 6, the good agreement between the present theory and the Low Density Wind Tunnel data is clearly evident. Induced pressures have also been measured on 5° cones in helium[26] in the range $M_1 = 16$ to 18, and $0.8 < \bar{\chi}_c < 1.6$. A best fit through the higher points of these data is $(p_2 - p_c)/p_c \approx 1 + 0.25\,\bar{\chi}_c$, and if we correct to a $\gamma = 1.4$ gas by the theoretical weak-interaction factor[18] $\gamma(\gamma - 1)$, we obtain $(p_2 - p_c)/p_c \approx 1 + 0.13\,\bar{\chi}_c$, which may be compared with the best fit for the present data, $(p_2 - p_c)/p_c \approx 1 + 0.12\,\bar{\chi}_c$.

Hole Size Effect

It has been shown by Talbot[1] and by Rayle,[9] and others, that the apparent pressure sensed by a static pressure orifice increases with the diameter of the orifice. The phenomenon is due to mixing between the stream passing over the surface and the fluid confined within the orifice and pressure tubulation; the momentum transferred by the mixing sets up currents in the fluid within the orifice which give rise to the increase in pressure.

Ideally, a static pressure orifice should be as small as possible, both to minimize this hole size effect and to provide a truly localized pressure measurement. However, in rarefied gas flow if a pressure orifice is made small enough one encounters another effect, known as thermal transpiration, which can also result in errors in pressure measurement. Thermal transpiration occurs, for example, when an orifice whose diameter is small compared to the mean free path separates two regions of gas at different temperatures.[10] In this case, the pressure ratio is given by

$$p_1/p_2 = \sqrt{T_1/T_2} \tag{1}$$

The static pressure orifices used in the present experiments were 0.010 in. in diameter. For an orifice of this size, the pressure increment due to momentum mixing is completely negligible. However, there is the possibility that thermal transpiration effects may be important, since the boundary layer is a region of strong temperature gradient, and many of the molecules which enter the orifice from the gas stream come from regions in the boundary layer which are at temperatures different from the gas within the orifice.

We can make a rough estimate of the magnitude of the thermal transpiration effect in the following way. We assume the boundary-layer characteristics to be given with sufficient accuracy by Howarth's analysis.[11] For an insulated cone, with $\sigma = 1$ and $\mu/\mu_2 = T/T_2$,

$$\delta = (5.0/\sqrt{3})(1 + 0.08M_2^2)\sqrt{\nu_2 x/u_2} \tag{2}$$

$$T/T_{aw} = \{1 + 0.2M_2^2[1 - (u^2/u_2^2)]\}/(1 + 0.2M_2^2) \tag{3}$$

Now, let us also assume that the velocity distribution in the boundary layer is linear in y. Then the temperature T_Λ at a distance Λ_w from the wall is given by

$$T_\Lambda/T_{aw} = \{1 + 0.2M_2^2[1 - (\Lambda_w^2/\delta^2)]\}/(1 + 0.2M_2^2) \tag{4}$$

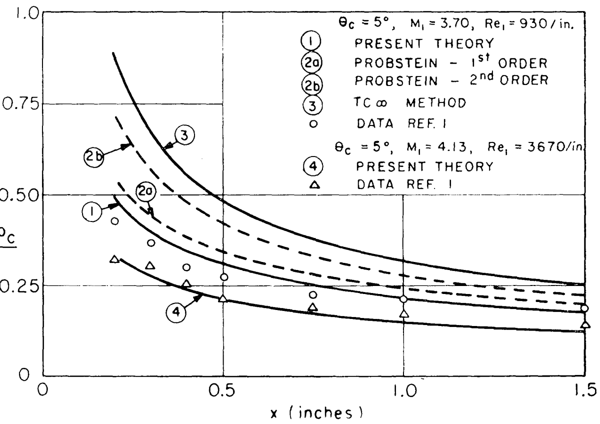

FIG. 5. 5° cone data, $M \sim 4$.

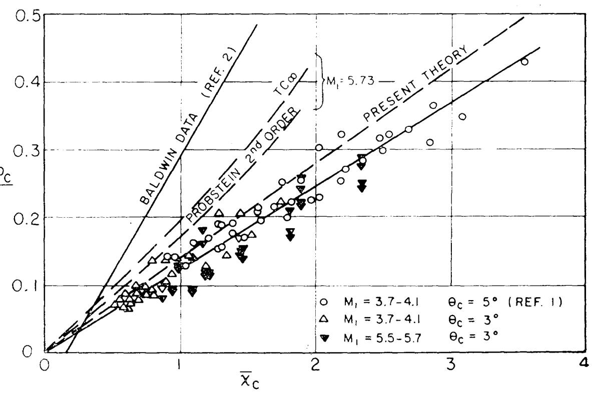

FIG. 6. Induced pressure increment vs. viscous interaction parameter $\bar{\chi}_c$.

We identify Λ_w with the mean free path of the gas at the wall.

As a specific example, let us take the following conditions:

$$M_2 = 5.5 \qquad x = 1 \text{ in.}$$
$$Re_2 = 10{,}000/\text{in.} \qquad T_{aw} = 270°\text{K.}$$
$$p_2 = 170\ \mu\text{Hg}$$

For these conditions $\Lambda_w = 0.011$ in., $\delta \approx 0.099$ in. Then from Eq. (1) we find $p_\Lambda/p_w = 0.994$, where we identify p_Λ as the pressure which we are attempting to measure and p_w as the pressure within the orifice which is presumably in error because of the thermal transpiration effect. It is seen that for this particular case the error is about 1/2 per cent. For the worst conditions, the error is found to be about 2 per cent. Actually, this analysis greatly overestimates the effect, since Eq. (1) is true only for $\Lambda_w/d \gg 1$. For the experiments $\Lambda_w/d \approx 1$, and in this range the pressure increment is less than 10 per cent of what it is in free molecule flow. One may conclude, therefore, that the pressures measured in the experiments were true static pressures, essentially uninfluenced by either momentum mixing or thermal transpiration hole size effects.

Appendix (A)

"Modified Tangent-Cone" Method

The assumptions usually made in the tangent-cone analysis for self-induced pressures are: (a) a region of inviscid flow exists between the outer edge of the boundary layer and the shock wave, and (b) the flow parameters, such as Mach Number, pressure, etc., at the edge of the boundary layer (subscript 2 in Fig. 1) can be obtained to satisfactory approximation by the tangent-cone (*TC*) method. The *TC* method consists of relating the local flow parameters on a body to the undisturbed flow ahead of the shock wave through conical flow theory (e.g., Taylor-Maccoll values), but using the local body inclination as the effective cone angle. In the case of self-induced pressures on a cone as shown in Fig. 1, the local effective cone angle is taken to be θ_2, the sum of the cone angle θ_c and the angle $\theta_\delta = \tan^{-1}(d\delta^*/dx)$.

Two computations are involved in utilizing the *TC* method for evaluation of self-induced pressures. First, the inviscid flow values must be obtained, for given effective cone angle θ_2, either from the exact solution (Kopal's Tables) or by one of several approximate methods[12, 13] which are available. Second, the boundary-layer displacement thickness must be evaluated, as a function of position along the cone surface, and here again several methods of varying accuracy and complexity are available. It will be noticed that the two computations are not independent. We are dealing with an interaction phenomenon—the boundary-layer growth determines the inviscid flow values at the outer edge of the boundary layer, but at the same time the rate of growth of the boundary layer is determined by these inviscid flow values. An accurate application of the *TC* method must include this interaction effect.

For the computations of the inviscid flow values, the exact Taylor-Maccoll results as computed by Kopal are employed. There are several supersonic and hypersonic flow approximations in analytic form which are accurate over different ranges of the similarity parameter $K_2 = M_1\theta_2$, but no single one is sufficiently accurate over the entire range of K_2 encountered in the tests reported here. The boundary-layer displacement thickness is calculated from the approximate formula of Monaghan,[14] which includes the effect of Prandtl Number and isothermal-wall heat transfer. It does not include the effects of pressure gradient or transverse curvature. To account in some measure for the variation in the external flow qualities along the outer edge of the boundary layer, local values of the external flow parameters are used to calculate M_2 and Re_{x_2}.

Monaghan's result, to which the Mangler[15] transformation correction has been applied, is

$$\left.\begin{aligned} \delta^*/x &= \sqrt{C/Re_{x_2}}\Big((\pi/2)\left\{(T_w/T_2) - [\sigma(\gamma-1)/4]M_2^2\right\} - \left\{1 + \sigma^{1/3}[(T_w - T_{aw})/T_2]\right\}\Big) \\ \tan\theta_\delta &= (d\delta^*/dx) \doteq (1/2)\cdot(\delta^*/x) \end{aligned}\right\} \qquad \text{(A-1)}$$

where $\quad T_{aw}/T_2 = 1 + [\sigma^{1/2}(\gamma - 1)M_2^2/2] \qquad$ (A-2)

and the Chapman-Rubesin C is defined by

$$C = (\mu'/\mu_c)/(T'/T_c) \qquad \text{(A-3)}$$

The viscosity μ' is evaluated at the intermediate T' given by

$$T'/T_c = (T_w/T_c) - 0.468\sigma^{1/3}[(T_w - T_{au})/T_c] - 0.273\sigma[(\gamma - 1)/2]M_c^2 \qquad \text{(A-4)}$$

However, instead of using the Sutherland law, as recommended by Monaghan, the Bromley-Wilke[16] values are used for μ'/μ_c, since the Sutherland law is less accurate at the low free-stream temperatures encountered in our tests. The actual wall temperature T_w is determined by experiment.

For a given free-stream condition (M_1, p_1, etc.), a set of values of θ_2 are chosen, and for each of these values a range of values of θ_δ are computed, using local free-stream conditions determined by the tangent-cone method and Kopal's Tables. The angle θ_δ is a function of x, for each selected value of θ_2. Since the value of x appropriate to a particular value of θ_2 is that for which $\theta_2 - \theta_\delta = \theta_c$, by cross plotting one can obtain θ_2 as a function of x, and, hence, p_2/p_c as a function of x.

Accuracy of the Method

The accuracy of the *TC* calculation of the inviscid flow has been examined by Ehret[17] and Lees,[18] by comparing pressure distributions on pointed ogives with exact values from the method of characteristics. The

TC method yields surface pressures which are slightly higher than the exact values, the difference depending on the distance from the vertex of the ogive. At the vertex the two methods, of course, give identical results; farther back the deviation may be of the order of a few per cent. It is found that the TC method also overestimates the pressure for blunt power-law bodies.[19]

In the calculation for self-induced pressures the effect of boundary-layer growth on the external inviscid flow is approximated by increasing the effective local cone angle by θ_δ. Order of magnitude arguments concerning the accuracy of this approximation have been given by Lees and Probstein.[20] The error involved in replacing the actual streamline inclination in the external flow by θ_δ is estimated to be of order $(\delta/x)^2$, where δ is the boundary-layer thickness. It also turns out that the neglect of pressure gradient across the boundary layer is also justified provided $(\delta/x)^2$ is small.

The variation in external flow properties along the outer edge of the boundary layer is partially taken into account by using local values for M_2, Re_2, p_2, etc. But it will be noted that the expression for $d\delta^*/dx$ [Eq. (A-1)] is only approximate, since the terms involving dM_2/dx, dT_2/dx, and dRe_2/dx have been neglected. It turns out that for the present calculations these terms contribute an increment of about 5 per cent at most to θ_δ, and their neglect is not serious.

Two important effects which have not been included in the boundary-layer analysis are the effect of transverse curvature and the direct effect of the self-induced pressure gradient on the density and velocity distributions within the boundary layer. Both the transverse curvature and the pressure gradient tend to thin the boundary layer, and thus result in smaller values for the induced pressure increment. The transverse curvature effect has been studied by Probstein and Elliott.[21] Probstein[22] concludes from his analysis, which is valid for small δ^*/r_c, that transverse curvature does not appreciably alter the boundary-layer displacement thickness. However, much of our data were in the range $\delta^*/r_c = 1$ to 3, and for these values the transverse curvature effect almost certainly cannot be neglected. An estimate of transverse curvature effect in very simple form is given by Hill, et al.,[23] in the form

$$(d\delta^*/dx)_{tc} = (d\delta^*/dx)/\sqrt{1 + 2\delta^*/r_c}$$

where δ^* is the displacement thickness calculated by theory, neglecting transverse curvature, and δ_{tc}^* the actual displacement thickness. This correction is probably not valid for values of δ^*/r_c as large as those of the present tests, but we may note that for $\delta^*/r_c = 1$, a reduction of about 40 per cent in the induced pressure is predicted.

Appendix (B)

Probstein's Analysis for the Self-Induced Pressure Effect

Probstein[22] considers a Taylor series expansion of the surface pressure in the form

$$(p_2 - p_c)/p_c = (p_1/p_c)\left\{[\partial(p_c/p_1)/\partial\theta]_{\theta=\theta_c} \cdot \theta_\delta + (1/2!)[\partial^2(p_c/p_1)/\partial\theta^2]_{\theta=\theta_c} \cdot \theta_\delta^2 + \ldots\right\} \quad \text{(B-1)}$$

Now, for $K_c < 1$, which is the range encountered in the present tests, the Lees hypersonic approximation is not accurate, so that the values for the derivatives in (B-1) obtained by Probstein cannot be used. Probstein suggests that for $K_c < 1$ the ratio p_1/p_c be evaluated from the Kopal Tables, but that the derivatives be evaluated from the von Kármán[24] slender body result. However, this result is also not sufficiently accurate. Guided by Van Dyke's suggestions[25] for combined supersonic-hypersonic similarity, we found that a formula of the form

$$p_c/p_1 = 1 + (A_1\gamma M_1^2\theta_c^2/2)\ln\left(A_2/\theta_c\sqrt{M_1^2 - 1}\right) \quad \text{(B-2)}$$

could be made to fit the Kopal values and the Van Dyke second-order theory values for p_c/p_1 over the range $0.14 < \theta_c\sqrt{M_1^2 - 1} < 0.3$; $0 < \theta_c < 0.13$ radians. The constants found were $A_1 = 1.52$, $A_2 = 2.85$. Expression (B-2) was used to calculate the derivatives in Eq. (B-1), and expression (A-1) was used to evaluate θ_δ and θ_δ^2, except that inviscid flow values M_c, Re_c, and T_c, were used instead of the local values M_2, Re_2, and T_2.

We found that it was necessary to include at least two terms in the series. For example, with $M_1 = 3.70$, $\theta_c = 5°$,

$$\left.\begin{aligned}(p_1/p_c)[\partial(p_1/p_c)/\partial\theta]_{\theta=\theta_c} &= 3.5\\ (p_1/p_c)[\partial^2(p_1/p_c)/\partial\theta^2]_{\theta=\theta_c} &= 17\end{aligned}\right\} \quad \text{(B-3)}$$

We also performed a numerical differentiation of a curve constructed from cross-plots of the Kopal entries and the 3° values calculated by second-order theory, and obtained the values 3.8 and 38 for the above derivatives. The first of these values may be more accurate than that given in Eq. (B-3). Not much accuracy can be claimed for either set, however.

The results of the Probstein analysis are shown in Figs. 4(b) and 5. The curves entitled "1st Order" were obtained using only the first term in the series (B-1), those entitled "2nd Order" using two terms. It can be seen that for small angle cones (i.e., small K_c) the convergence of the series is slow. This slow convergence is already evident at $K_c = 1$, as can be seen from examination of the functions presented in reference 22.

As a check on the Probstein analysis, we also evaluated two induced pressure distributions by what we have called the "TC_∞" Method. In this method the boundary-layer slope θ_δ is calculated from the inviscid flow values T_c, M_c, and Re_c, rather than the local values of these quantities, but the tangent cone method with the Kopal values rather than the Probstein series is used to evaluate the pressure. The TC_∞ method, of course, gives the values that the Probstein method should converge to. As is evident in Figs. 4(b) and 5, the use of two terms in the Probstein series provides a fairly good approximation. But Probstein's method is not very useful for $K_c < 1$, because it is difficult to obtain accurate values for the required derivatives.

References

[1] Talbot, L., *Viscosity Corrections to Cone Probes in Rarefied Supersonic Flow at Nominal Mach Number of 4*, NACA TN 3219, 1954.

[2] Baldwin, L. C., *Viscous Effects on Static Pressure Distribution or a Slender Cone at a Nominal Mach Number of 5.8*, GALCIT Hypersonic Wind Tunnel Memo No. 28, June 14, 1955.

[3] Maslach, G. J., and Sherman, F. S., *Design and Testing of an Axisymmetric Hypersonic Nozzle for a Low Density Wind Tunnel*, University of California Engineering Project Report HE-150-134, Series 23, Issue 17, February, 1956.

[4] Van Dyke, M. D., *Practical Calculation of Second Order Supersonic Flow Past Nonlifting Bodies of Revolution*, NACA TN 2744, 1952.

[5] Kopal, Z., *Tables of Supersonic Flow of Air Around Cones*, Tech. Report No. 1, Massachusetts Institute of Technology, Cambridge, 1947.

[6] Schaaf, S. A., Hurlbut, F. C., Talbot, L., and Aroesty, J., *Viscous Interaction Experiments at Low Reynolds Numbers*, ARS Journal, p. 527, July, 1959.

[7] Kendall, J. M., Jr., *An Experimental Investigation of Leading-Edge Shock Wave-Boundary Layer Interaction at Mach 5.8*, Journal of the Aeronautical Sciences, Vol. 24, No. 1, pp. 47–56, January, 1957.

[8] Blumer, C. B., Bradfield, W. S., and Scott, C. J., *The Effect of Cone Tip Blunting on the Supersonic Conical Laminar Boundary Layer*, Rosemont Aero. Lab. Engineering Memo 29, University of Minnesota, March, 1954.

[9] Rayle, R. E., Jr., *An Investigation of the Influence of Orifice Geometry on Static Pressure Measurements*, M.S. Thesis in Mechanical Engineering, Massachusetts Institute of Technology, 1949.

[10] Loeb, L. B., *Kinetic Theory of Gases*, 2nd Ed., McGraw-Hill Book Company, Inc., New York, 1934.

[11] Howarth, L., *Concerning the Effect of Compressibility on Laminar Boundary Layers and Their Separation*, Proc. Royal Soc. A, No. 1036, Vol. 194, pp. 16–42, 1948.

[12] Lees, L., *Note on the Hypersonic Similarity Law for an Unyawed Cone*, Journal of the Aeronautical Sciences, Vol. 18, No. 10, pp. 700–702, October, 1951.

[13] Probstein, R. F., and Bray, K. N. C., *Hypersonic Similarity and the Tangent-Cone Approximation for Unyawed Bodies of Revolution*, Journal of the Aeronautical Sciences, Vol. 22, No. 1, pp. 66–68, January, 1955.

[14] Monaghan, R. J., *An Approximate Solution of the Compressible Laminar Boundary Layer on a Flat Plate*, ARC R&M No. 2760, Great Britain, 1953.

[15] Howarth, L., (Ed.), *Modern Developments in Fluid Dynamics, High Speed Flow*, Vol. 1, Oxford University Press, p. 382, 1953.

[16] Bromley, L. A., and Wilke, C. R., *Viscosity Behavior of Gases*, Industrial and Engineering Chemistry, Vol. 143, p. 1641, July, 1951.

[17] Ehret, D. M., *Accuracy of Approximate Methods for Predicting Pressures on Pointed Nonlifting Bodies of Revolution in Supersonic Flow*, NACA TN 2764, August, 1952.

[18] Lees, L., *Hypersonic Flow*, Fifth International Aeronautical Conference, Los Angeles, pp. 241–276, 1955. Also available as GALCIT Publication No. 404.

[19] Kubota, T., *Inviscid Hypersonic Flow over Blunt-Nosed Slender Bodies*, Paper presented at 1957 Heat Transfer and Fluid Mechanics Institute, California Institute of Technology, Pasadena, Calif., June 19–21, 1957. See also GALCIT Hypersonic Research Project, Memorandum 40, June 25, 1957, and Lees, L., *Recent Developments in Hypersonic Flow*, Jet Propulsion, November, 1957.

[20] Lees, L., and Probstein, R. F., *Hypersonic Viscous Flow Over a Flat Plate*, Princeton University, Aero. Engrg. Lab. Report No. 195, April 20, 1952.

[21] Probstein, R. F., and Elliott, D., *The Transverse Curvature Effect in Compressible Axially Symmetric Laminar Boundary Layer Flow*, Journal of the Aeronautical Sciences, Vol. 23, No. 3, pp. 208–244, March, 1956.

[22] Probstein, R. F., *Interacting Hypersonic Laminar Boundary Layer Flow Over a Cone*, Technical Report AF 2798/1, Division of Engineering, Brown University, Providence, R.I., March, 1955.

[23] Hill, J. A. F., et al., *Mach Number Measurements in High-Speed Wind Tunnels*, AGARDograph 22, October, 1956.

[24] von Kármán, T., *The Problem of Resistance in Compressible Fluids*, Proc. 5th Volta Congress, pp. 210–271, Rome, 1935.

[25] Van Dyke, M. D., *A Study of Hypersonic Small-Disturbance Theory*, NACA TR 1194, 1954.

[26] Erickson, W. D., *Study of Pressure Distributions on Simple Sharp-Nosed Models at Mach Numbers From 16 to 18 in Helium Flow*, NACA TN 4113, October, 1957.

Some Effects of Sound-Reduction Devices on a Turbulent Jet

(*Continued from page 722*)

One cannot, on the strength of the present experiment alone, determine whether the turbulence values u'/U_j yield a sufficiently complete working index of the noise radiating efficiency of a jet. Still, reasons have been adduced to hope that the evaluation of the noise generating strength of a jet by its turbulence levels will prove adequate for engineering purposes. To establish the point, the type of measurements reported here should be made on a number of different nozzles with known noise generating efficiency.

What has been said in no way obviates the need for a more informative (and more difficult) study which might relate a more exact measure of the noise source strength with some integral property of the turbulent region.

References

[1] Corcos, G. M., *Some Measurements Bearing on the Principle of Operation of Jet Silencing Devices*, Douglas Aircraft Company, Inc., Report No. SM-23114, March, 1958.

[2] Lighthill, M. J., *On Sound Generated Aerodynamically, I, General Theory*, Proc. Roy. Soc., Series A, Vol. 211, p. 564, 1952.

[3] Liepmann, H. W., *Aspects of the Turbulence Problem*, ZAMP, Vol. III, p. 407, 1952.

[4] Unpublished Douglas Aircraft Company, Inc., and NACA data.

[5] Lighthill, M. J., *On Sound Generated Aerodynamically, II, Turbulence As a Source of Sound*, Proc. Roy. Soc., Series A, Vol. 222, p. 1, 1954.

[6] Tyler, J. M., *Jet Noise*, SAE Preprint No. 287, 1954.

[7] Lassiter, L. W., and Hubbard, H. H., *Experimental Studies From Subsonic Jets in Still Air*, NACA TN 2757, 1952.